Highly selective Fe3+ and F−/H2PO4− sensor based on a water-soluble cationic pillar[5]arene with aggregation-induced emission characteristic

Hong Yao, Qi Zhou, Jiao Wang, Yan-Yan Chen, Xiao-Tong Kan, Tai-Bao Wei, You-Ming Zhang, Qi Lin

PII:	S1386-1425(19)30605-5
DOI:	https://doi.org/10.1016/j.saa.2019.117215
Article Number:	117215
Reference:	SAA 117215
To appear in:	*Spectrochimica Acta Part A: Molecular and Biomolecular Spectroscopy*
Received date:	13 December 2018
Revised date:	25 April 2019
Accepted date:	26 May 2019

Please cite this article as: H. Yao, Q. Zhou, J. Wang, et al., Highly selective Fe3+ and F−/H2PO4− sensor based on a water-soluble cationic pillar[5]arene with aggregation-induced emission characteristic, Spectrochimica Acta Part A: Molecular and Biomolecular Spectroscopy, https://doi.org/10.1016/j.saa.2019.117215

Highly Selective Fe^{3+} and $F^-/H_2PO_4^-$ Sensor Based on a Water-soluble Cationic Pillar[5]arene with Aggregation-Induced Emission Characteristic

Hong Yao*, Qi Zhou, Jiao Wang, Yan-Yan Chen, Xiao-Tong Kan, Tai-Bao Wei*,
You-Ming Zhang, and Qi Lin*

Key Laboratory of Eco-Environment-Related Polymer Materials, Ministry of Education of China, Key Laboratory of Polymer Materials of Gansu Province, College of Chemistry and Chemical Engineering, Northwest Normal University, Lanzhou, Gansu 730070, PR China

---

E-mail: yhxbz@126.com; weitaibao@126.com; linqi2004@126.com.

Abstract:

A water-soluble cationic pillar[5]arene (**CWP5**) without lager conjugated construction was first reported as a novel pillar[5]arene-based aggregation-induced emission luminogen (AIEgen), which showed a remarkable aggregation-induced emission (AIE) with the concentration increasing. The AIE effect of **CWP5** has affected by different solvent, it had the lowest critical aggregation concentration (CAC) value and highest fluoresence emission intensity in DMSO solution. Simultaneously, **CWP5** can serve as a chemosensor for the successively fluorescent detection of Fe^{3+} and $F^-/H_2PO_4^-$ with high sensitivity and selectivity. A rewritable portable test kit made from **CWP5** provides a possibility to on-site detection and manufacture of encryption and decryption materials.

Keywords:

chemosensor; AIEgens; self-assembly; ion detection; portable test kit; encryption and decryption materials

1. Introduction

Fluorescent sensors with aggregation-induced emission (AIE) attributes have attracting much attention since the concept of AIE was first proposed [1-2]. AIE is a phenomenon that AIE luminogens (AIEgens) are weakly or even non-emission when the luminogens are molecularly dispersed in solvent, but exhibit a robust augmentation of fluorescent emission in aggregates [3-5] as a result of restriction of intramolecular motions and relax through radiative pathways [6-7]. AIE-based sensors for ions [8], organic volatiles [9], toxic gases [10], small molecules [11], biological molecules [12] and so forth have experienced rapid development by virtue of its fast responsiveness, superb sensitivity and simple operation [13]. Despite a variety of AIEgens have been reported, such as derivatives of tetraphenylethene (TPE) [14], tetraphenylpyrazine (TPP) [15], silole [16], arylbenzene [17-18], pyrrole [19] and some metal complexes [20], which usually consist of lager conjugated structure. There are still enthusiastic interest of scientists worldwide in exploring novel sensors with remarkable AIE feature in recent years.

Pillar[n]arenes, as a new class of macrocyclic host compounds, have received extensive attention. They exhibit intriguing and peculiar properties in fluorescent supramolecular aggregates [21-22], host-guest recognition [23-24] and biological applications [25] due to their rigid and symmetrical architecture, facile modification and existence of multiple self-assembly driving forces: hydrophobic/hydrophilic interactions, $\pi\cdots\pi$ interactions, C-H$\cdots\pi$ interactions, cation$\cdots\pi$ interactions, and H-bond etc [26-27]. These merits may endow pillar[n]arenes with AIE properties through construction of supramolecular systems. Common construction strategies of pillar[n]arenes-based AIEgens are on one hand introducing conventional AIEgens, such as TPE, into pillar[n]arenes structure by modifying the benzene rings on pillar[n]arenes [28-29], on the other hand utilizing TPE as guest molecules to assemble with pillar[n]arene [30-31]. Even though pillar[n]arenes possessing AIE properties without conventional AIEgens have been rarely reported. Our research group has reported a novel bispillar[5]arene with AIE attribute which can further used to mercury (Ⅱ) detection [32], but development of simple pillar[5]-based AIEgens is still an urgent and important task.

Detection of biologically essential or environmentally related ions is important in biological study and environment inspection [33]. For example, iron ion (Fe^{3+}) as one of the most essential trace elements has an important role in biological processes, e.g., oxygen transport, DNA synthesis and the growth of biological cells. But the extra of iron ion will cause vomiting, diarrhea and damage to the intestine, even more seriously leading Parkinson's and Alzheimer's [34]. Moreover, small amounts of fluoride (F^-) intake may be beneficial for bone strength and prevent dental caries, while excess fluoride may cause kidney failure, skeletal fluorosis, even death [35]. $H_2PO_4^-$ as a central component of nucleic acids (DNA and RNA) plays a crucial role in life system. Meanwhile phosphate fertilizers are frequently used in agriculture and drug-related industries [36]. Therefore, exploiting new sensors for the sensitive and selective detection and developing convenient on-site detection of above mentioned ions have attracted our attention for a long time.

Based on our previous research and longstanding interest in pillar[5]arene chemistry and sensors for ions recognition, in order to develop newer AIEgen sensor, we have designed and synthesized a simple water-soluble cationic pillar[5]arene (**CWP5**) by connecting trimethylamine group with bromopillar[5]arene through nuleophilic substitution reaction [37]. Fortunately, we have surprisingly found that although **CWP5** did not have lager conjugated construction, it exhibited aggregation-induced emission (AIE) in aggregates with increasing of the concentration, which suggested that **CWP5** is a new kind of pillar[5]arene-based AIEgen. Interestingly, the AIE effect of **CWP5** has affected by different solvent. Furthermore, this simple water-soluble cationic pillar[5]arene could be used as a AIE-based sensor for successively fluorescence detection of Fe^{3+} and F^-/$H_2PO_4^-$.

2. Experimental section

2.1 Materials physical methods

All reagents and starting materials were obtained from commercial suppliers and used as received unless otherwise noted. All cations (Fe^{3+}, Ca^{2+}, Mg^{2+}, Co^{2+}, Ni^{2+}, Zn^{2+}, Ba^{2+}, Cd^{2+}, Cu^{2+}, Hg^{2+}, Pb^{2+}, Cr^{3+}, Eu^{3+}, Ag^{+}, Al^{3+}, La^{3+}, perchlorate salts, 0.1 M, in water) and anions (tetrabutylammonium salt of anions: F^-, Cl^-, Br^-, I^-, Ac^-, OH^-, HSO_4^-, $H_2PO_4^-$, ClO_4^-; sodium azide salt of anion: N_3^-; sodium salt of anion:CN^-, $P_2O_7^{4-}$, CO_3^{2-}, NO_3^-, S^{2-} and SCN^-, 0.1 M, in water) were purchased from Alfa Aesar and used as received.

2.2 Physical methods

Nuclear magnetic resonance (NMR) spectra were recorded on Varian Mercury 400 and Varian Inova 600 instruments. The X-ray diffraction analysis (XRD) was performed in a transmission mode with a Rigaku RINT2000 diffractometer equipped with graphite monochromated CuKa radiation (λ = 1.54073 Å). The morphologies of complex were characterized using field emission scanning electron microscopy (FE-SEM, JSM-6701F) at an accelerating voltage of 8 kV. The infrared spectra were performed on a Digilab FTS-3000 Fourier transform-infrared spectrophotometer. Fluorescence spectra were recorded on a Shimadzu RF–5301spectrofluorophotometer.

2.3 Synthesis of CWP5 and reference compound R.

The water-soluble cationic pillar[5]arene (**CWP5**) was synthesized using a method described in our previous work [35, 37]. Meanwhile, we also synthesized compound R as a control (Scheme S1). Moreover, the target compound were characterized by ^{1}H NMR, ^{13}C NMR, and ESI-MS (Fig. S1-S3).

3. Results and Discussion

3.1 Critical Aggregation Concentration (CAC) Determination of CWP5

The fluorescence (FL) emission behaviour of **CWP5** in different solvent that include DMSO, DMF, EtOH, H_2O and MeCN were examined by the fluorescence emission spectra. As the Fig. 1a shown, **CWP5** shows the relatively highest fluorescence emission intensity in DMSO solution.

(Insert Fig. 1)

To further investigate the impact of solvent on aggregation effect of **CWP5**, concentration depended fluorescence emission spectra was used to determine the critical aggregation concentration (CAC) of **CWP5** [38] in H_2O, DMSO, and EtOH (Fig. S4). A double logarithmic plot of specific fluorescence intensity versus concentration was obtained, presenting a fluorescence intensity transition. With the increase of the concentration, a remarkable uprush in the fluorescence intensity was observed, indicating that **CWP5** may self-assemble into supramolecular system to produce aggregation-induced emission (AIE). Using the increased slope, the CAC values of **CWP5** in H_2O, DMSO, and EtOH were calculated as 0.20 mg/mL, 0.07 mg/mL and 0.10 mg/mL, respectively (Fig. 1b, c, d). These results demonstrated that **CWP5** have lowest CAC value in DMSO solution. In light of these, we selected DMSO as the solvent for the next experiments due to **CWP5** have highest fluorescence emission intensity and lowest CAC value in DMSO, and the quantum yield of the probe in DMSO was calculated to be 0.49 (Eq. S1).

Meanwhile, we also found that the reference compound R had no obvious fluorescence emission at the same condition (Fig. S6), which revealed that the aggregation-induced emission of **CWP5** was related to the columnar structure of pillar[5]arene.

3.2 Fluorescent response behavior of CWP5 towards cations

In order to investigate application of pillar[5]arene-based AIEgen as sensors, we primarily investigated the sensing properties of **CWP5** towards cations by adding 10 equiv. of various cations into the **CWP5**. Interestingly, as shown in Fig. 2, only Fe^{3+} could induce the fluorescence of **CWP5** completely to quench, and the other tested cations could not induce a similar response. It was also essential to explore the selectivity of **CWP5** towards Fe^{3+} by performing interference studies. Negligible interference with any of the coexisting cations showed **CWP5** can highly selectively sense for Fe^{3+} (Fig. 3).

(Insert Fig. 2)

(Insert Fig. 3)

To further investigated the performance of the **CWP5** for Fe^{3+} detection, the fluorescence emission profile of the **CWP5** was monitored in the presence of increasing concentrations of Fe^{3+} ions (0 - 9.5 equiv.). A completely quenching of the fluorescence could be evidently perceived from Fig. 4. The detection limit for Fe^{3+} was estimated to be 7.49×10^{-8} M based on $3\delta/S$ method (Fig. S8), indicating CWP5 has high sensitivity for Fe^{3+} than other sensing systems (Table S1). Moreover, the association constant (K_a) of **CWP5** with Fe^{3+} was about 1.11×10^6 M^{-1} and the stoichiometry between CWP5 and Fe^{3+} 1:2, which was obtained from the intercept and slope of the linear fit of fluorescence titration experiment as shown in (Fig. S9). Simultaneously, the obtained Job's plot (Fig. S10) also proved that CWP5 and Fe^{3+} exhibit a 1:2 binding mode.

(Insert Fig. 4)

3.3 Fluorescent response behavior of CWP5-Fe^{3+} for anions

From those above results, the AIE-active **CWP5** could act as a detector for Fe^{3+} with high selectivity and sensitivity. Then, the recognition property of **CWP5-Fe^{3+}** for anions has been further investigated by adding 20 equiv. various anions into **CWP5-Fe^{3+}** solution. As a result (Fig. 5), the fluorescence of **CWP5-Fe^{3+}** turned on again upon adding F^- or $H_2PO_4^-$ into the **CWP5-Fe^{3+}**. Moreover, we also carried out fluorescence emission titration experiment, with an increasing amount of F^- or $H_2PO_4^-$, and found emission peak at 446 nm gradually increased (Fig. S11a, S13a). The detection limit of **CWP5-Fe^{3+}** for $F^-/H_2PO_4^-$ was 2.53×10^{-8} M and 5.04×10^{-8} M, respectively (Fig. S11b, S13b), which was also calculated by $3\delta/S$ method. The Job's plot between CWP5-Fe^{3+} and $F^-/H_2PO_4^-$ showed 1:3 and 1:2 stoichiometry, respectively (Fig. S12, S14). Given the above, **CWP5-Fe^{3+}** achieved high sensitivity during successively detection for anions, and superior than most previous sensors (Table S1).

(Insert Fig. 5)

3.4 The possible self-assembly and recognition mechanism of CWP5

As a proof of ion detection properties of this pillar[5]arene-based AIEgen, the self-assembly mechanism of **CWP5** was first investigated using concentration-dependent ^{1}H-NMR, 2D-NOESY NMR, concentration-dependent UV-Vis experiment, XRD and SEM. To begin with, the concentration-dependent ^{1}H-NMR of **CWP5** were carried out (Fig. S15). The resonance signals of H_a and H_b shifted downfield and H_b became broadened. Besides, the signals of proton H_f and H_g displayed slightly upfield shifts. Then, 2D-NOESY NMR of the **CWP5** was performed to investigate the relative spatial positions of protons. When the concentration of **CWP5** was 5 mM, there was no correlation signals observed (Fig. S16 a). As the concentration of **CWP5** increased to 80 mM, correlation signals (A, B, C, D in Fig. 6) appeared between protons H_a, H_b and H_f, H_g. These results indicated that the partial positively charged trimethylammonium head of **CWP5** threaded into the cavity of the other **CWP5**, and further self-assembled into supramolecular system, while the intramolecular motion is restricted in the self-assembly system and an aggregation-induced emission (AIE) was observed. To further justify the aggregation of CWP5 was occurred, the concentration-dependent UV-Vis absorption spectra of CWP5 was also measured. As Fig. S5 shown, a neatly linear relationship between absorbance (A) and the concentration was obtained with a slope of 0.12 at low concentration, which neatly fitted the beers law and manifested no obvious aggregation between the solute molecules. However, with the concentration increased, a remarkable change in the absorbance was observed as the slope of the curve increased to 2.02, indicating the foramtion of CWP5 aggregates and the CAC value reached 10^{-5} M. The XRD pattern of **CWP5** showed peaks at $2\theta = 21.98^{\circ}, 25.02^{\circ}, 32.72^{\circ}$ corresponding to the d-spacing 4.04, 3.56 and 2.73 Å (Fig. S17a), which confirmed that the exo-wall π-π stacking and C-H···π interaction existed [39]. Meanwhile, the morphological features of **CWP5** were studied by SEM, showing a curving ribbon-like structure (Fig. 7a). These above results indicated that the **CWP5** self-assembled into supramolecular system and leaded to aggregation-induced emission (AIE) at relatively high concentration.

(Insert Fig. 6)

(Insert Fig. 7)

Then the recognition mechanism of **CWP5** for Fe^{3+} was verified by IR spectroscopy, XRD and SEM. Comparing the IR spectrum of **CWP5-Fe^{3+}** and **CWP5** (Fig. S17b), we found that the stretching vibration absorption peaks of =C-H, C=C on benzene ring of **CWP5** were changed into the 3023, 2966 and 2926 cm^{-1} respectively after addition of Fe^{3+} into CWP5. Besides, the vibration absorption peaks of the C-O-C and CH_2 adjacent to benzene ring of CWP5 were also obviously changed. In addition, Fe^{3+} is easy to bind with the π electrons of pillar[5]arene groups through cation-π interactions due to Fe^{3+} ion has odd electron and high ionic strength [40]. These results indicated that the CWP5 coordinated with Fe^{3+} via the cation-π interactions [26]. Moreover, the peaks at $2\theta = 21.98^{\circ}, 25.02^{\circ}$ (d = 4.04, 3.56 Å) was disappeared after adding Fe^{3+} into CWP5 (Fig. S17a), which confirmed that the tight exo-wall π-π stacking was destroyed and the aggregates of CWP5 disassembled because Fe^{3+} combined with CWP5 by cation-π interaction. The SEM characterized that the morphological of CWP5 transformed from a curving ribbon-like structure to a short rod-like structure in the present of Fe^{3+} (Fig. 7), this phenomenon further proof the above point. These above experimental phenomenon turned out that **CWP5** combined with Fe^{3+} and generated **CWP5-Fe^{3+}** via the cation-π interactions, and exo-wall π-π stacking between **CWP5** was destroyed. The disassembly process of **CWP5** supramolecular system reduced the AIE fluorescence of **CWP5** and even completely quenching. As we know, both F^- and $H_2PO_4^-$ have a strong binding ability with Fe^{3+} to form compounds $[Fe(H_2PO_4)_3]$ and $[FeF_6^{3-}]$, respectively. In consequence, the aggregation-induced emission (AIE) of **CWP5** was recovered when the added F^-/ $H_2PO_4^-$ competed Fe^{3+} with **CWP5** and the supramolecular system of **CWP5** restructured.

(Insert Scheme 1)

3.5 Practical Application

Finally, we investigated the practical application of this novel pillararene-based AIE sensor. As shown in Fig. 8, an untreated silica gel plate can be served as a rewritable portable test kit, when we writing on this test kit using a writing brush inked with DMSO solution of CWP5(1.0 mM), a significant blue handwriting can be observed under UV lamp at 365 nm. In addition, the handwriting can be erased by Fe^{3+} water solution (1.0×10^{-4} M) and reappeared by $F^-/H_2PO_4^-$ aqueous solution (1.0×10^{-4} M), which is very convenient for on-site detection. The rewritable portability of **CWP5** can be used to achieve novel encryption and decryption materials.

(Insert Fig. 8)

4. Conclusion

A novel simple water-soluble cationic pillar[5]arene-based AIEgen (**CWP5**) was reported, which showed aggregation-induced emission (AIE) with the increase of concentration. The AIE principle was explained as that partial positively charged trimethylammonium groups of **CWP5** threaded into the cavity of the other **CWP5** and further self-assembled into supramolecular system through exo-wall π-π stacking and C-H···π interaction. This novel pillar[5]arene-based AIEgen can be used as fluorescence sensor for sensitive and selective detection for Fe^{3+} and $F^-/H_2PO_4^-$. A rewritable portable test kit was fabricated with **CWP5** for on-site detection and encryption and decryption technology.

Acknowledgments

This work was supported by the National Natural Science Foundation of China (No. 21661028; 21662031; 21574104), the Program for Changjiang Scholars and Innovative Research Team in University of Ministry of Education of China (IRT 15R56).

References

[1] Y. N. Hong, J. W. Y. Lam, B. Z. Tang, Aggregation-induced emission, Chem. Soc. Rev. 40 (2011) 5361-5388.

[2] Y. Ma, M. Cametti, Z. Džolić, S. M. Jiang, AIE-active bis-cyanostilbene-based organogels for quantitative fluorescence sensing of CO_2 based on molecular recognition principles, J. Mater. Chem. C. 6 (2018) 9232-9237.

[3] J. D. Luo, Z. L. Xie, J. W. Y. Lam, L. Cheng, H. Y. Chen, C. F. Qiu, H. S. Kwok, X. W. Zhan, Y. Q. Liu, D. B. Zhu, Aggregation-induced emission of 1-methyl-1,2,3,4,5-pentaphenylsilole, Chem. Commun. 18 (2001) 1740-1741.

[4] Q. Zhao, Y. Liu, Tunable photo-luminescence behaviors of macrocvcle-containing polymer networks in the solid-state, Chem. Commun. 54 (2018) 6068-6071.

[5] F. K. Merkt, T. J. J. Müller, Synthesis and electronic properties of expanded 5-(hetero)aryl-thien-2-yl substituted 3-ethynyl quinoxalines with AIE characteristics, Sci. China Chem. 61 (2018) 1-16.

[6] M. Gao, B. Z. Tang, Fluorescent sensors based on aggregation-induced emission: recent advances and perspectives, Acs Sens. 2 (2017) 1382-1399.

[7] S. W. Cheng, T. Han, T. Y. Huang, B. Z. Tang, G. S. Liou, High-performance electrofluorochromic devices based on aromatic polyamides with AIE-active tetraphenylethene and electro-active triphenylamine moieties, Polym. Chem. 9 (2018) 4364-4373.

[8] Q. Y. Li, X. J. Wu, X. L. Huang, Y. J. Deng, N. J. Chen, D. D. Jiang, L. L. Zhao, Z. H. Lin, Y. G. Zhao, Tailoring the fluorescence of AIE-Active metal-organic frameworks for aqueous sensing of metal ions, ACS Appl. Mater. Interfaces. 10 (2018) 3801-3809.

[9] W. Y. Dong, Y. Y. Pan, M. Fritsch, U. Scherf, High sensitivity sensing of nitroaromatic explosive vapors based on polytriphenylamines with AIE-active tetraphenylethylene side groups, J. Polym. Sci., Part A: Polym. Chem. 53 (2015) 1753-1761.

[10] M. Gao, S. W. Li, Y. H. Lin, Y. Geng, X. Ling, L. C. Wang, A. J. Qin, B. Z. Tang, Fluorescent light-up detection of amine vapors based on aggregation-induced emission, ACS Sens. 1 (2016) 179-184.

[11] J. B. Qiu, Y. X. Chen, S. J. Jiang, H. Y. Guo, F. F. Yang, A fluorescent sensor based on aggregation-induced emission: highly sensitive detection for hydrazine and application in living cell imaging, Analyst. 143 (2018) 4298-4305.

[12] F. Ji, C. Wang, H. M. Wang, G. L. Liu, B. L. Chen, L. G. Hu, G. B. Jiang, M. Y. Song, Y. Liang, Tetrabromobisphenol A (TBBPA) exhibits specific antimicrobial activity against gram-positive bacteria without detectable resistance, Chem. Commun. 53 (2017) 3512-3515.

[13] D. Li, J. Liu, R. T. Kwok, Z. Liang, B. Z. Tang, J. Yu, Supersensitive detection of explosives by recyclable AIE luminogen-functionalized mesoporous materials, Chem. Commun. 48 (2012) 7167-7169.

[14] N. W. Sun, K. X. Su, Z. W. Zhou, Y. Yu, X. Z. Tian, D. M. Wang, X. G. Zhao, H. W. Zhou, C. H. Chen, AIE-active polyamide containing diphenylamine-TPE moiety with superior electrofluorochromic performance, ACS Appl. Mater. Interfaces. 10 (2018) 16105-16112.

[15] M. Chen, L. Z. Li, H. Nie, J. Q. Tong, L. L. Yan, B. Xu, J. Z. Sun, W. J. Tian, Z. J. Zhao, A. J. Qin, B. Z. Tang, Tetraphenylpyrazine-based AIEgens: facile preparation and tunable light emission, Chem. Sci. 6 (2015) 1932-1937.

[16] Z. J. Zhao, B. R. He, B. Z. Tang, Aggregation-induced emission of siloles, Chem. Sci. 6 (2015) 5347-5365.

[17] J. Yang, X. Q. Gu, W. T. Su, X. Y. Hao, Y. J. Shi, L. Y. Zhao, D. F. Zou, G. W. Yang, Q. Y. Li, J. H. Zou, (2-(4-Bromophenyl)ethene-1,1,2-triyl)tribenzene with aggregation induced emission for ablation of HeLa cells, Mater. Chem. Front. 2 (2018) 1842-1846.

[18] Y. H. Zhang, W. Q. Xu, L. W. Kong, B. R. Han, Z. X. Cai, J. B. Shi, B. Tong, Y. P. Dong, B. Z. Tang, Turn-on fluorescent probe with aggregation-induced emission characteristic for polyazoles, Mater. Chem. Front. 2 (2018) 1779-1783.

[19] K. Li, Y. Y. Liu, Y. Y. Li, Q. Feng, H. W. Hou, B. Z. Tang, 2,5-bis(4-alkoxycarbonylphenyl)-1,4-diaryl-1,4-dihydropyrrolo[3,2-b]pyrrole (AAPP) AIEgens: tunable RIR and TICT characteristics and their multifunctional applications, Chem. Sci. 8 (2017) 7258-7267.

[20] B. Gui, N. Yu, Y. Meng, F. Hu, C. Wang, Immobilization of AIEgens into metal-organic frameworks: Ligand design, emission behavior, and applications, J. Polym. Sci., Part A: Polym. Chem. 55 (2017) 1809-1817.

[21] L. L. Tan, Y. L. Zhu, Y. H. Jin, W. Zhang, Y. W. Yang, Highly CO_2 selective pillar [n] arene-based supramolecular organic frameworks, Supramol. Chem. 30 (2018) 648-654.

[22] T. Kakuta, T. A. Yamagishi, T. Ogoshi, Stimuli-responsive supramolecular assemblies constructed from pillar[n]arenes, Acc. Chem. Res. 51 (2018) 1656-1666.

[23] H. T. Zhu, J. Q. Liu, B. B. Shi, H. H. Wang, Z. W. Mao, T. Z. Shan, F. H. Huang, Pillararene-based host−guest recognition facilitated magnetic separation and enrichment of cell membrane proteins, Mater. Chem. Front. 2 (2018) 1475-1480.

[24] L. Shao, J. F. Sun, B. Hua, F. H. Huang, An AIEE fluorescent supramolecular cross-linked polymer network based on pillar[5]arene host-guest recognition: Construction and application in explosive detection, Chem. Commun. 54 (2018) 4866-4869.

[25] D. Wu, Y. Li, J. Shen, Z. Z. Tong, Q. L. Hu, L. P. Li, G. C. Yu, Supramolecular chemotherapeutic drug constructed from pillararene-based supramolecular amphiphile, Chem. Commun. 54 (2018) 8198-8201.

[26] Y. M. Zhang, W. Zhu, W. J. Qu, K. P. Zhong, X. P. Chen, H. Yao, T. B. Wei, Q. Lin, Competition of cation-π and exo-wall π-π interactions: a novel approach to achieve ultrasensitive response, Chem. Commun. 54 (2018) 4549-4552.

[27] Q. Lin, K. P. Zhong, J. H. Zhu, L. Ding, J. X. Su, H. Yao, T. B. Wei, Y. M. Zhang, Iodine controlled pillar[5]arene-based multiresponsive supramolecular polymer for fluorescence detection of cyanide, mercury, and cysteine, Macromolecules. 50 (2017) 7863-7871.

[28] B. Han, L. P. Zhu, X. Wang, M. Bai, J. Z. Jiang, Conformation-controlled emission of AIE luminogen: a tetraphenylethene embedded pillar[5]arene skeleton, Chem. Commun. 54 (2018) 837-840.

[29] L. W. Ma, S. Wang, C. P. Li, D. R. Cao, T. Li, X. Ma, Photo-controlled fluorescence on/off switching of a pseudo[3]rotaxane between an AIE-active pillar[5]arene host and a photochromic bithienylethene guest, Chem. Commun. 54 (2018) 2405-2408.

[30] X. Y. Jin, N. Song, X. Wang, C. Y. Wang, Y. Wang, Y. W. Yang, Monosulfonicpillar[5]arene: synthesis, characterization, and complexation with tetraphenylethene for aggregation-induced emission, Sci. Rep. 8 (2018) 4035-4043.

[31] J. Zhou, B. Hua, L. Shao, H. Feng, G. C. Yu, Host-guest interaction enhanced aggregation-induced emission and its application in cell imaging, Chem. Commun. 52 (2016) 5749-5752.

[32] Q. Lin, X. M. Jiang, X. Q. Ma, J. Liu, H. Yao, Y. M. Zhang, T. B. Wei, Novel bispillar[5]arene-based AIEgen and its' application in mercury (II) detection, Sens. Actuators, B. 272 (2018) 139-145.

[33] M. Xue, Y. Yang, X. D. Chi, X. Z. Yan, F. H. Huang, Development of pseudorotaxanes and rotaxanes: from synthesis to stimuli-responsive motions to applications, Chem. Rev. 115 (2015) 7398-7501.

[34] A. Dou, L. B. Yang, X. D. Fang, Q. Yin, M. D. Li, J. Li, M. Y. Wang, A. X. Zhu, Q. Q. Xu, Two luminescent lanthanide-organic frameworks containing bithiophene groups for selective detection of nitrobenzene and Fe^{3+}, CrystEngComm. 20 (2018) 3609-3619.

[35] Q. Lin, Y. Q. Fan, P. P. Mao, L. Liu, J. Liu, Y. M. Zhang, H. Yao, T. B. Wei, Pillar[5]arene-based supramolecular organic framework with multi-guest detection and recyclable separation properties, Chem. Eur. J. 24 (2017) 777-783.

[36] M. S. Han, D. H. Kim, Naked-eye detection of phosphate ions in water at physiological pH: a remarkably selective and easy-to-assemble colorimetric phosphate-sensing probe, Angew. Chem. 41 (2010) 3809-3811.

[37] Q. Lin, L. Liu, F. Zheng, P. P. Mao, J. Liu, Y. M. Zhang, H. Yao, T. B. Wei, A water-soluble pillar[5]arene-based chemosensor for highly selective and sensitive fluorescence detection of L-methionine, RSC Adv. 7 (2017) 34411-34414.

[38] G. D. Liang, F. Ren, H. Y. Gao, Q. Wu, F. M. Zhu, B. Z. Tang, Bioinspired fluorescent nanosheets for rapid and sensitive detection of organic pollutants in water, ACS Sens. 1 (2016) 1272-1278.

[39] X. D. Chi, M. Xue, Y. Yao, F. H. Huang, Redox-responsive complexation between a pillar[5]arene with mono(ethylene oxide) substituents and paraquat, Org. Lett. 15 (2013) 4722-4725.

[40] A. K. Pearson, P. Kao, A. P. O'Mullane, A. I. Bhatt, Investigating the effect of ionic strength on the suppression of dendrite formation during metal electrodeposition, Phys. Chem. Chem. Phys. 19 (2017) , 14745-14760.

List of Figures and Schemes:

Fig. 1. (a) Fluorescence emission spectra of CWP5 (1.0 mM) in various solvent. A double logarithmic plot of fluorescence intensity versus concentration of CWP5 in (b) H_2O, (c) DMSO, and (d) EtOH (λ_{ex} = 380 nm).

Fig. 2. (a) Fluorescence emission spectra of CWP5 (2.0×10^{-4} M, in DMSO at λ_{ex} = 380 nm) upon addition of 10.0 equiv. various cations. (b) photograph showing the corresponding color changes of CWP5 with various cations under UV lamp (365 nm).

Fig. 3. Changes in fluorescence emission spectra of CWP5 (2.0×10^{-4} M, in DMSO at λ_{ex} = 380 nm, λ_{em} = 446 nm) upon addition of 10.0 equiv. various cations (0.1 M, in water) in the presence of 10.0 equiv. Fe^{3+} (0.1 M, in water).

Fig. 4. Fluorescent spectrum of CWP5 (2.0×10^{-4} M, in DMSO at λ_{ex} = 380 nm) in the presence of different concentration of Fe^{3+}. Inset: A plot of fluorescent intensity depending on the concentration of Fe^{3+} in the range from 0 to 9.5 equivalents.

Fig. 5. Fluorescent spectra of CWP5-Fe^{3+} (2.0×10^{-4} M, with 10 equiv. Fe^{3+}, in DMSO at λ_{ex} = 380 nm) in the presence of 20 equiv. various anions (F^-, Cl^-, Br^-, I^-, Ac^-, OH^-, HSO_4^-, $H_2PO_4^-$, ClO_4^-, N_3^-, CN^-, $P_2O_7^{4-}$, CO_3^{2-}, NO_3^-, S^{2-} and SCN^-, 0.1 M, in water).

Fig. 6. 2D NOESY NMR spectrum (600 MHz, 298K) of 80 mM CWP5 in DMSO-d_6 solution.

Fig. 7. Representative SEM images of (a) CWP5 and (b) CWP5-Fe^{3+} .

Fig. 8. Writing and erasing experiment on silica gel plate. The photographs were taken under UV lamp (365 nm) at room temperature.

Scheme 1. The possible self-assembly and recognition mechanism of CWP5.

Figures

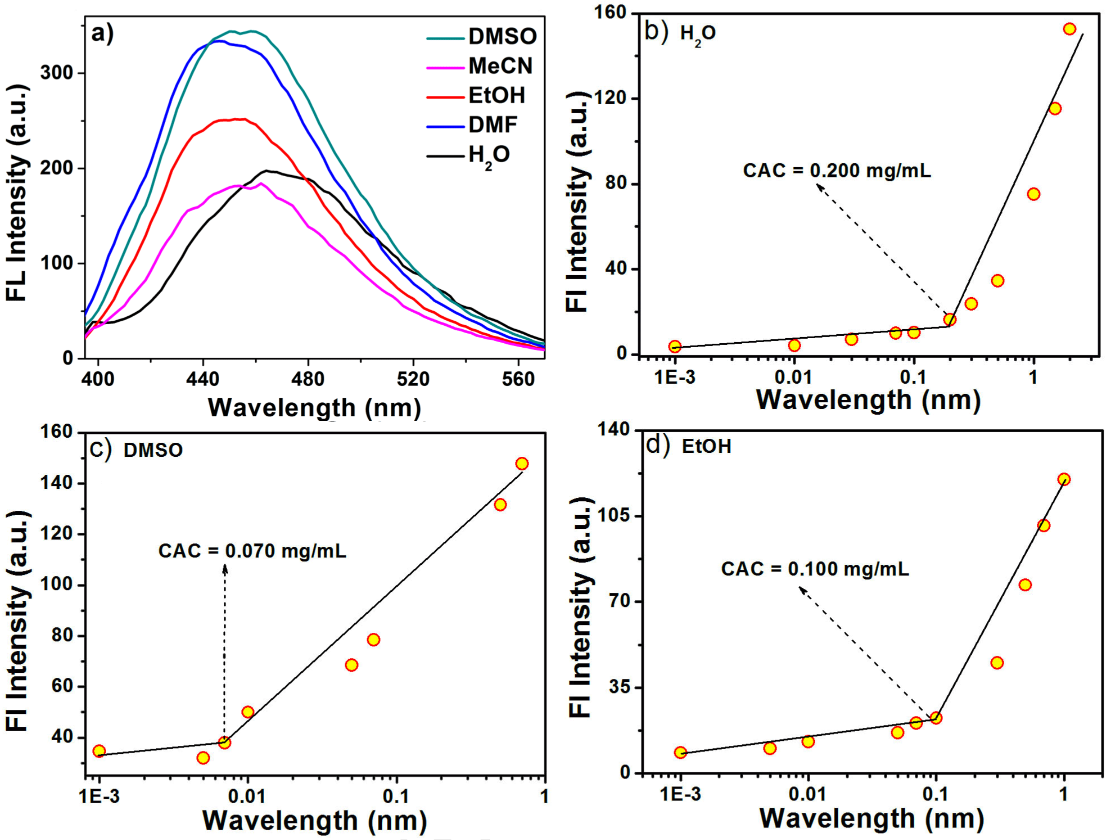

Fig. 1 (a) Fluorescence emission spectra of CWP5 (1.0 mM) in various solvent. A double logarithmic plot of fluorescence intensity versus concentration of CWP5 in (b) H_2O, (c) DMSO, and (d) EtOH (λ_{ex} = 380 nm).

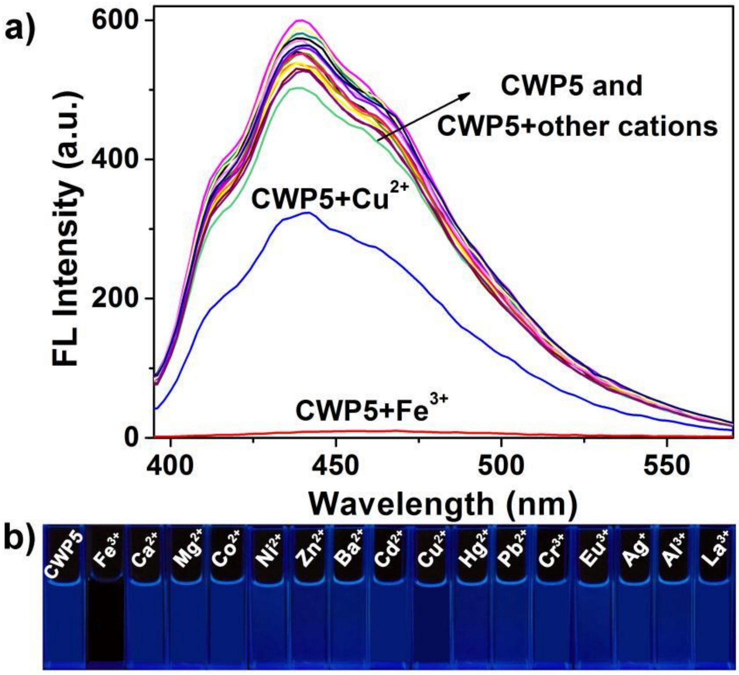

Fig. 2 (a) Fluorescence emission spectra of CWP5 (2.0×10^{-4} M, in DMSO at λ_{ex} = 380 nm) upon addition of 10.0 equiv. various cations. (b) photograph showing the corresponding color changes of CWP5 with various cations under UV lamp (365 nm).

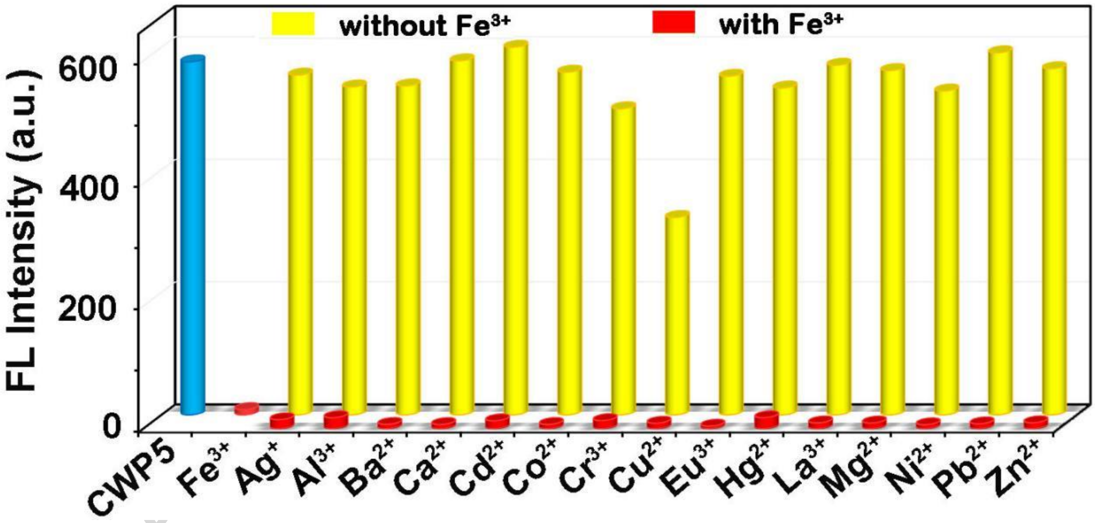

Fig. 3 Changes in fluorescence emission spectra of CWP5 (2.0×10^{-4} M, in DMSO at λ_{ex} = 380 nm, λ_{em} = 446 nm) upon addition of 10.0 equiv. various cations (0.1 M, in water) in the presence of 10.0 equiv. Fe^{3+} (0.1 M, in water).

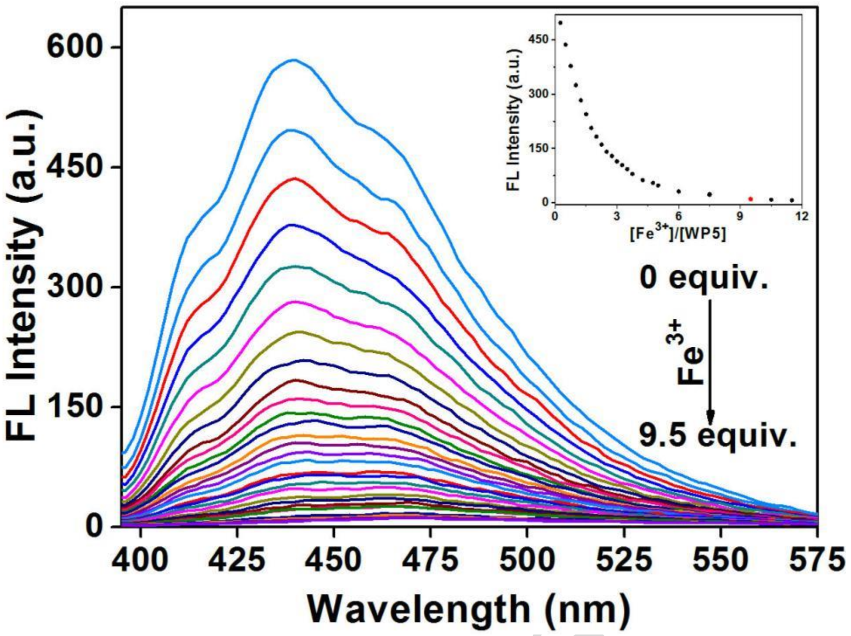

Fig. 4 Fluorescent spectrum of CWP5 (2.0 × 10^{-4} M, in DMSO at λ_{ex} = 380 nm) in the presence of different concentration of Fe^{3+}. Inset: A plot of fluorescent intensity depending on the concentration of Fe^{3+} in the range from 0 to 9.5 equivalents.

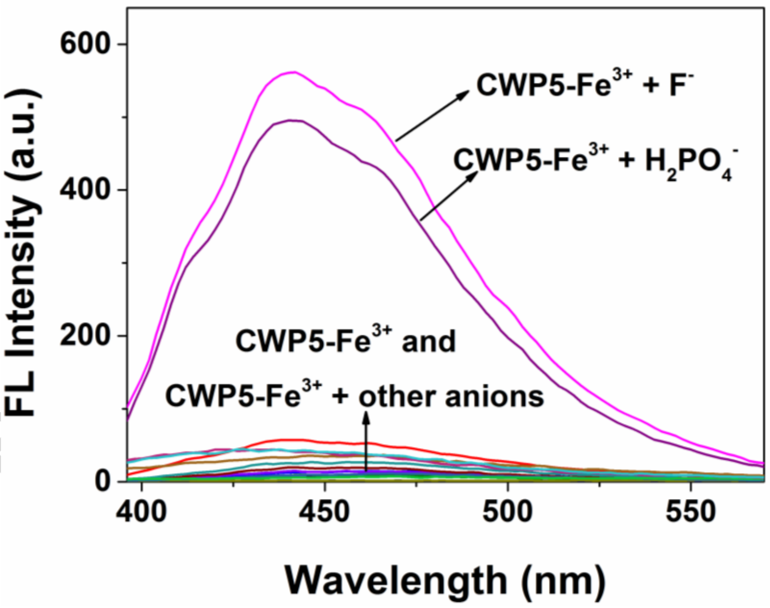

Fig. 5 Fluorescent spectra of CWP5-Fe^{3+} (2.0 × 10^{-4} M, with 10 equiv. Fe^{3+}, in DMSO at λ_{ex} = 380 nm) in the presence of 20 equiv. various anions (F^-, Cl^-, Br^-, I^-, Ac^-, OH^-, HSO_4^-, $H_2PO_4^-$, ClO_4^-, N_3^-, CN^-, $P_2O_7^{4-}$, CO_3^{2-}, NO_3^-, S^{2-} and SCN^-, 0.1 M, in water).

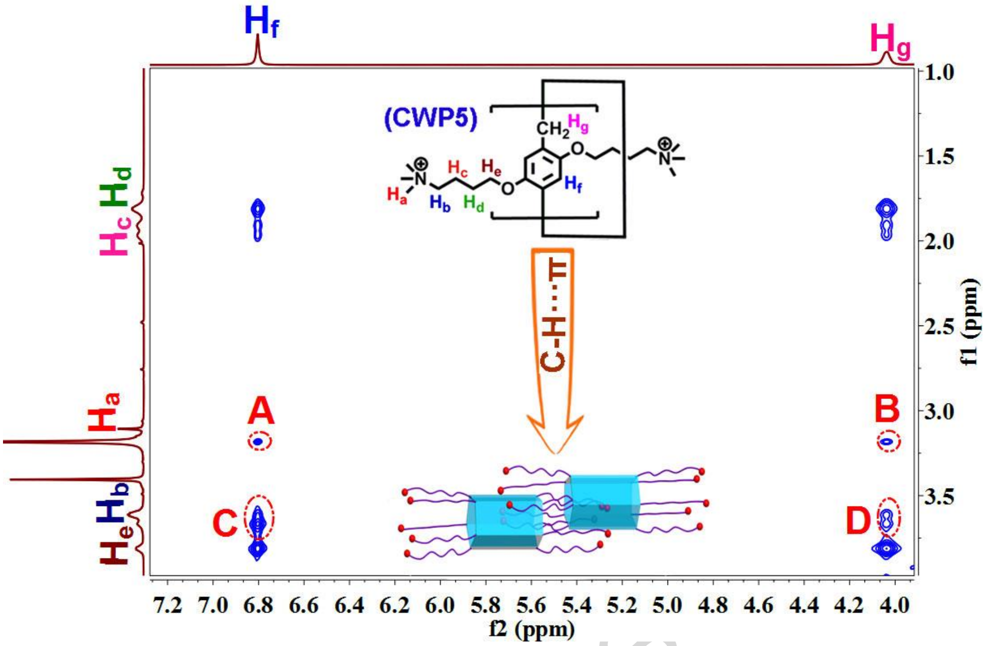

Fig. 6 2D NOESY NMR spectrum (600 MHz, 298K) of 80 mM CWP5 in DMSO-d_6 solution.

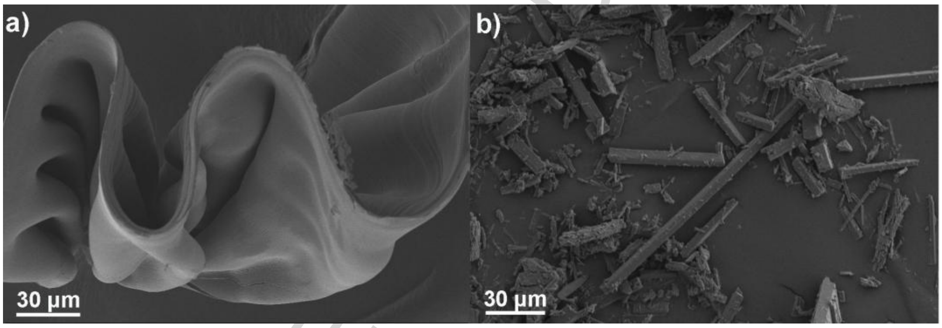

Fig. 7 Representative SEM images of (a) CWP5 and (b) CWP5-Fe^{3+} .

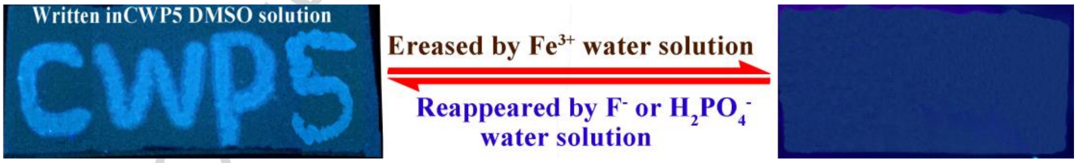

Fig. 8 Writing and erasing experiment on silica gel plate. The photographs were taken under UV lamp (365 nm) at room temperature.

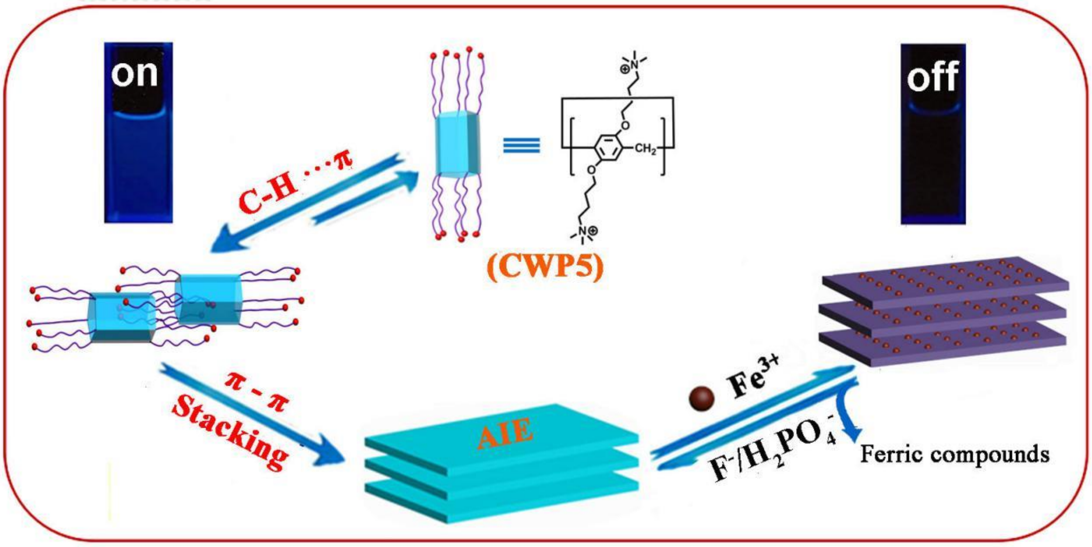

Scheme 1. The possible self-assembly and recognition mechanism of CWP5.

Graphical Abstract:

In this paper, a water-soluble cationic pillar[5]arene (**CWP5**) without large conjugation construction was first reported as a new pillar[5]arene-based aggregation-induced emission luminogen (AIEgen). **CWP5** exhibited bright blue fluorescence emission in aggregate state due to self-assembly of **CWP5** driving by exo-wall π-π stacking and C-H···π interaction. Simultaneously, **CWP5** could successively fluorescent detection of Fe^{3+} and $F^-/H_2PO_4^-$ with high sensitivity and selectivity. We also prepared a rewritable portable test kit using **CWP5** that provides a possibility to on-site detection and manufacture of encryption and decryption materials.

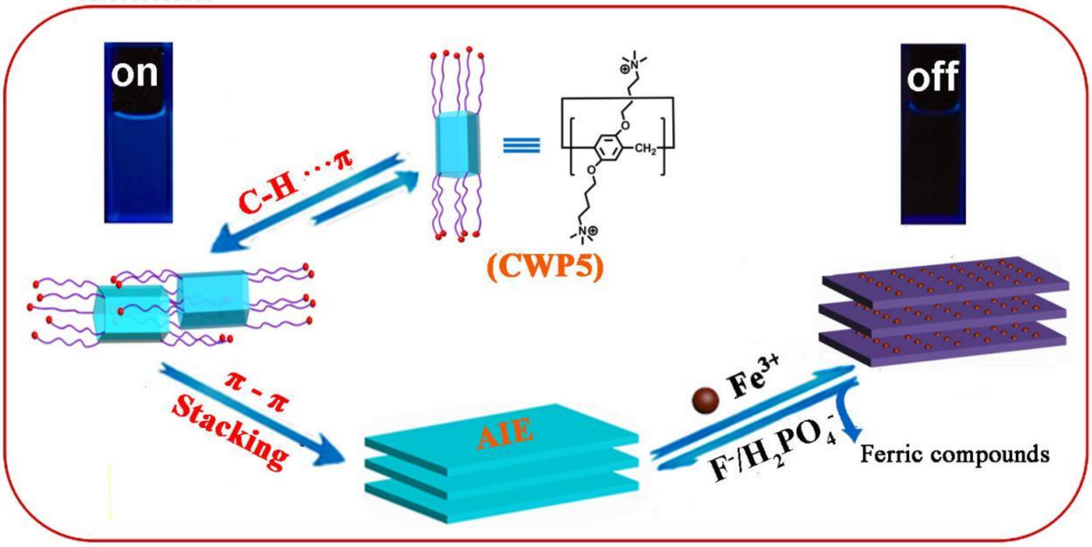

Research Highlights:

1 A novel water-soluble pillar[5]arene-based AIEgen (**CWP5**) was reported.

2 **CWP5** without large conjugation construction exhibited strong AIE fluorescence.

3 AIE-active **CWP5** could successively detect Fe^{3+} and $F^-/H_2PO_4^-$.

4 A portable test kit made from **CWP5** could achieve convenient on-site detection.

5 **CWP5** give a possibility for manufacture encryption and decryption materials.

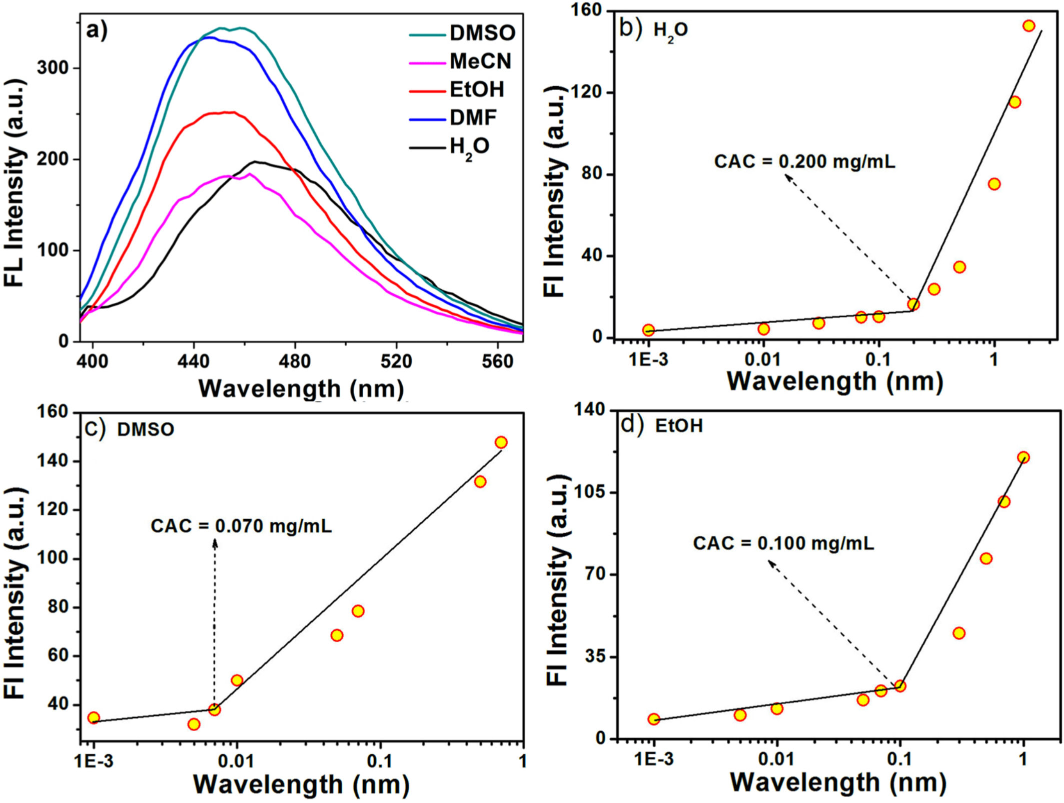
a)
DMSO
MeCN
EtOH
DMF
H_2O
FL Intensity (a.u.)
Wavelength (nm)
0
100
200
300
400
440
480
520
560
b) H_2O
CAC = 0.200 mg/mL
Fl Intensity (a.u.)
Wavelength (nm)
0
40
80
120
160
1E-3
0.01
0.1
1
C) DMSO
CAC = 0.070 mg/mL
Fl Intensity (a.u.)
Wavelength (nm)
40
60
80
100
120
140
160
1E-3
0.01
0.1
1
d) EtOH
CAC = 0.100 mg/mL
Fl Intensity (a.u.)
Wavelength (nm)
0
35
70
105
140
1E-3
0.01
0.1
1

Figure 1

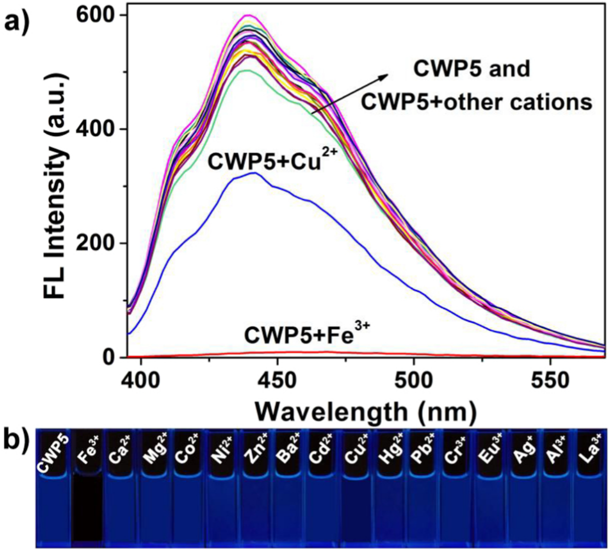
a)
FL Intensity (a.u.)
0
200
400
600
400
450
500
550
Wavelength (nm)
CWP5 and
CWP5+other cations
CWP5+Cu^{2+}
CWP5+Fe^{3+}
b)
CWP5
Fe^{3+}
Ca^{2+}
Mg^{2+}
Co^{2+}
Ni^{2+}
Zn^{2+}
Ba^{2+}
Cd^{2+}
Cu^{2+}
Hg^{2+}
Pb^{2+}
Cr^{3+}
Eu^{3+}
Ag^{+}
Al^{3+}
La^{3+}

Figure 2

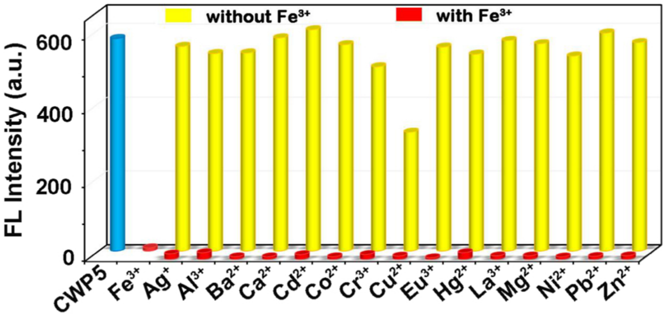
without Fe^{3+}
with Fe^{3+}
FL Intensity (a.u.)
600
400
200
0
CWP5
Fe^{3+}
Ag^{+}
Al^{3+}
Ba^{2+}
Ca^{2+}
Cd^{2+}
Co^{2+}
Cr^{3+}
Cu^{2+}
Eu^{3+}
Hg^{2+}
La^{3+}
Mg^{2+}
Ni^{2+}
Pb^{2+}
Zn^{2+}

Figure 3

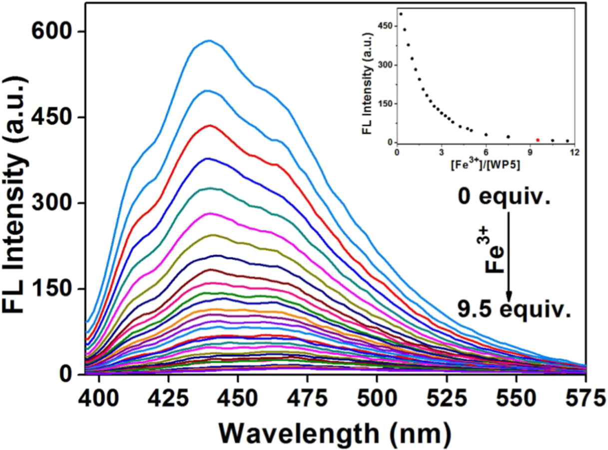
FL Intensity (a.u.)
600
450
300
150
0
400
425
450
475
500
525
550
575
Wavelength (nm)
FL Intensity (a.u.)
450
300
150
0
0
3
6
9
12
[Fe^{3+}]/[WP5]
0 equiv.
Fe^{3+}
9.5 equiv.

Figure 4

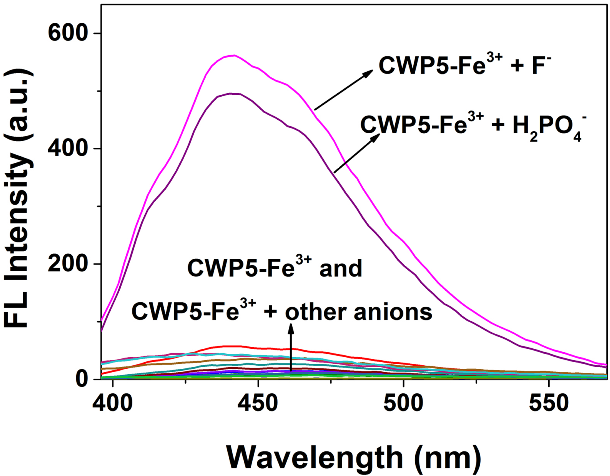
CWP5-Fe^{3+} + F$^-$
CWP5-Fe^{3+} + H$_2$PO$_4^-$
CWP5-Fe^{3+} and
CWP5-Fe^{3+} + other anions
FL Intensity (a.u.)
Wavelength (nm)
0
200
400
600
400
450
500
550

Figure 5

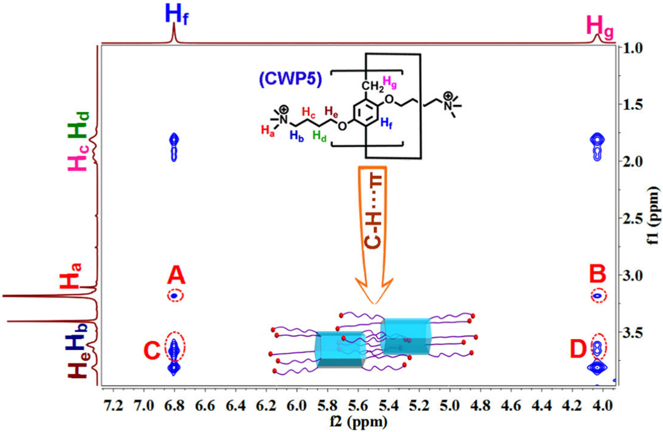H_f
H_g
(CWP5)
CH_2 H_g
H_c H_e
H_a H_b H_d H_f
C-H···π
A
B
C
D
H_c H_d
H_a
H_e H_b
7.2 7.0 6.8 6.6 6.4 6.2 6.0 5.8 5.6 5.4 5.2 5.0 4.8 4.6 4.4 4.2 4.0
f2 (ppm)
1.0 1.5 2.0 2.5 3.0 3.5
f1 (ppm)

Figure 6

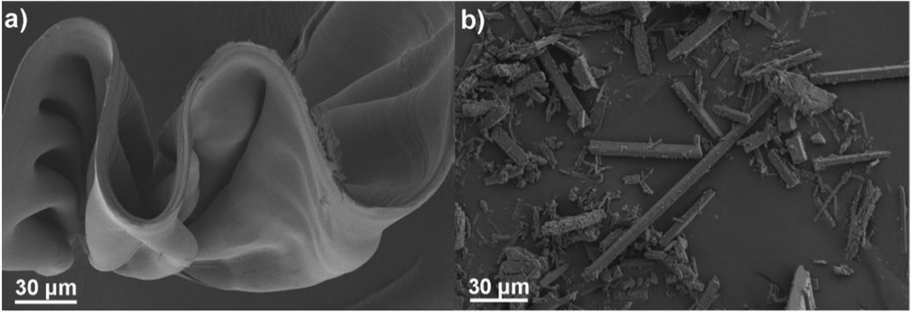

Figure 7

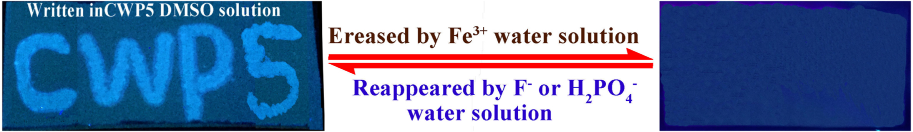
Written inCWP5 DMSO solution
CWP5
Ereased by Fe^{3+} water solution
Reappeared by F^- or $H_2PO_4^-$ water solution

Figure 8